water

MDPI

Article

Hydrochemical and Formation Mechanism Studies of Groundwater in Quaternary Aquifer in a Northern Plain of China: An Example of Beijing Plain

Sarah Fatim Camara *, Jinjun Zhou * and Yongxiang Zhang

Faculty of Architecture, Civil and Transportation Engineering, Beijing University of Technology, Beijing 100124, China; yxzhang@bjut.edu.cn

* Correspondence: sarahcamara@yahoo.com (S.F.C.); zhoujj@bjut.edu.cn (J.Z.)

Abstract: Beijing Plain is a very active part of Beijing city regarding the socio-economic and human activities of the region. Over the past four decades, Beijing's economic development and the continuous drought for nearly 10 years in the 2000s have negatively impacted the groundwater quantity and quality. Therefore, it is necessary to investigate the present situation of groundwater chemistry in this region to develop a comprehensive database and orientation for future research on groundwater quality evaluation. Mathematical statistics, Piper's trilinear diagram, Gibbs plots, the ion ratio method and PHREEQC software 3.7.3 were used to analyze the groundwater hydrogeochemical characteristics and formation mechanisms of the quaternary aquifers of the Beijing Plain area. Hydrogeochemical results indicated that the groundwater is slightly alkaline, with pH values ranging from 6.76 to 8.65 and an average value of 7.92. The order of major cations in groundwater was $Ca^{2+} > Na^{+} > Mg^{2+} > K^{+}$ with average values of 66.54 mg/L, 50.58 mg/L, 23.78 mg/L, and 1.81 mg/L, respectively, while the order of major anions was $HCO_3^{-} > SO_4^{2-} > Cl^{-}$ with average values of 284.89 mg/L, 52.1 mg/L and 35.5 mg/L, respectively. The groundwater chemical types are Mg-Ca-Cl-HCO_3, Na-Ca-HCO_3, Mg-Ca-HCO_3 and Mg-Na-HCO_3. Research on the main influencing factors and PHREEQC hydrogeochemical inverse simulations results along the four pathways selected confirmed that rock weathering with sulfate, silicate and carbonate rock mineral dissolution and Na^{+}, Mg^{2+} and Ca^{2+} ion reaction exchange influenced groundwater hydrogeochemical characteristics of the quaternary aquifers of the Beijing Plain area. Understanding the formation mechanisms of hydrogeochemistry in quaternary plains provides guidance for future studies and, through suggestions and case studies, facilitates decision-making by policy-makers on the sustainable management of groundwater resources.

Keywords: quaternary aquifer; hydrogeochemical characteristics; groundwater quality; Beijing Plain; PHREEQC

Citation: Camara, S.F.; Zhou, J.; Zhang, Y. Hydrochemical and Formation Mechanism Studies of Groundwater in Quaternary Aquifer in a Northern Plain of China: An Example of Beijing Plain. *Water* **2024**, *16*, 2060. https://doi.org/10.3390/w16142060

Academic Editor: Zbigniew Kabala

Received: 27 May 2024
Revised: 10 July 2024
Accepted: 18 July 2024
Published: 21 July 2024

1. Introduction

Water is the most basic natural resource, an important strategic resource for economic development, and is essential for human life [1,2]. Most of the available freshwater on Earth is stored as groundwater. In fact, groundwater is the main resource of available water supply, representing 30% of the world's freshwater or 2.5% of the total global water storage with a total volume of 23.4×10^6 km^3 [3]. Over the past four decades, precisely from 1978 to 2011, rapid urbanization, population growth and climate variability have caused a serious water scarcity situation in Beijing [4,5]. The city's reliance on limited groundwater resources has led to over-extraction, causing significant environmental issues such as land subsidence and depletion of water tables [6]. According to the data on water from the Beijing Statistical Yearbook for the period from 1999 to 2011, and other research studies, continuous drought and over-exploitation induced the decline of the groundwater level table from −11.7 m to −24.3 m [7–9]. During the period from 2005 to 2015, the China Geological Survey conducted a national groundwater quality survey [10] that covered an area of 440 km^2 and

nearly 300,000 monitoring wells across the country. Survey results showed no optimistic overall situation of groundwater quality in China. Indicators like Mn (manganese), Fe (iron), TDS (total dissolved solids), F (fluoride), I (iodide), and As (arsenic) in groundwater were greater than the limit of Class III of the groundwater quality standard, accounting for 33.9%, 28.5%, 23.0%, 15.0%, 14.0%, and 7.83% of the total number of survey points, respectively. Moreover, terrain has a significant impact on the land occupation and activity nature of a specific area. The importance of slope may affect the infiltration of water or any other surface material into aquifers. Therefore, it is necessary and important to investigate the hydrogeochemical characteristics and formation mechanisms of groundwater in order to establish the current status of the regional groundwater environment, provide updated data for groundwater quality monitoring and ensure multi-sector sustainable development.

As established in the previous statements and scholars' research papers, regional flow systems, chemical composition and formation mechanisms of groundwater are influenced by many factors, such as climate, topography, lithology and human activities [11–15]. According to several studies, the main mechanism controlling the hydrogeochemical processes of groundwater is hydrometamorphism, and ion exchange also plays an important role [16–18]. The main ions in groundwater are related to the geological structure and lithology of the aquifer. Some researchers have studied the hydrogeochemical processes and related formation causes of groundwater through different methods; for example, Ren et al. [19] used hydrogeochemical and multivariate statistical techniques. The results showed that in northern China, NO_3^- and TH concentrations were primary pollution factors in the region with intensive human activity because of high concentrations over the standard rates. Other scholars combined basic hydrogeochemistry with mathematical statistics to analyze the evolution of groundwater chemistry [20,21]. Simulating hydrogeochemical models is also a common method for studying the chemical processes of groundwater. Hydrogeochemical models can be used to analyze the existence of various components in groundwater and simulate solute transport and chemical reactions [22], which are commonly used in the PHREEQC software developed by the U.S. Geological Survey [23]. Xie et al. [24] showed through PHREEQC inverse simulation that the salinization of groundwater in the Datong Basin is mainly controlled by silica-aluminate hydrolysis, cation exchange and evaporite dissolution. Liwen Huang et al. [25] used PHREEQC software reverse simulation to confirm that the formation process causing high fluorine content in the groundwater of the Hotan area is mainly the dissolution of fluorite, and precipitation of, e.g., calcite, can also promote the dissolution of fluorite.

The quaternary groundwater of Beijing Plain is an essential water supply source for agriculture, industries and domestic activities. Groundwater parameters such as manganese, iron, and total hardness seriously exceed the standard limits, which might greatly influence the development of the region and the health of residents [26]. A few recent studies have been conducted on the subject in this region. In this paper, hydrogeochemical methods and statistical methods are combined to deeply investigate the statistical characteristics of chemical parameters and groundwater chemical types in the quaternary groundwater of the Beijing Plain and determine the sources of the major groundwater ion elements. In addition, an inverse simulation technique was performed using PHREEQC software to gain a better understanding of the current phenomenon and exchanges within the aquifer. This study provides a data basis for monitoring and sustainable management of the groundwater resources in Beijing City.

2. Study Area

2.1. Physical Geography Overview

The city of Beijing is located at longitude 115.7°~117.4° E and latitude 39.4°~41.6° N. The city stretches across 160 km from east to west and 176 km from north to south with the center at latitude 39°54′20″ north and longitude 116°25′29″ east. With an area of 16,410 km², Beijing is located in the northern part of the North China Plain, bordering Tianjin to the east, and the rest of the city is bordered by the Hebei province. The Beijing Plain lies to the

south-east of Beijing and forms part of the North China Plain with the Jundu Mountains to the north, the Xishan Mountains to the west and the Great North China Plain to the east and south [27]. The research area covers approximately 6300 km² (excluding the Yanqing basin) and includes the plains of 15 administrative districts: Dongcheng, Xicheng, Haidian, Chaoyang, Fengtai, Mentougou, Shijingshan, Fangshan, Tongzhou, Shunyi, Changping, Daxing, Huairou, Pinggu and Miyun, representing approximately 40% of the total area of Beijing (Figure 1). The Beijing Plain area is subject to a warm, semi-humid, semi-arid continental temperate monsoon climate with wide temperature variations and four distinct seasons. The average annual temperature is 14.7 °C and the average annual rainfall is 585 mm [28]. Beijing belongs to the Haihe River basin because of its watershed, with a developed river system and main and secondary rivers. The five main river systems are the Daqing River, the Yongding River, the Northern Canal, the Chaobai River and the Jiyun Canal [29].

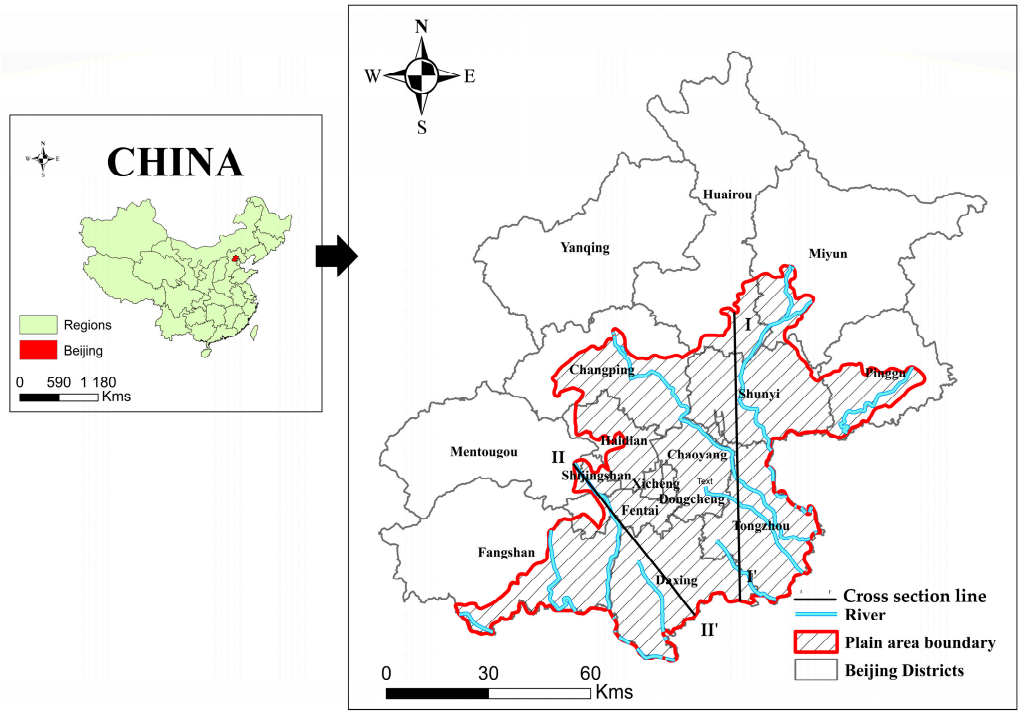

Figure 1. Study area location map.

2.2. Geological and Hydrogeological Overview

Based on the distribution of the stratigraphic lithology [30,31] and the groundwater burial conditions in the research area [32], in conjunction with the current situation of groundwater exploitation and use, the strata of the Beijing Plain can be divided into seven main categories according to the cause of the stratigraphic formation, namely plain fill, clay, cobble and gravel, clay, sand and gravel, clay, and red clay. The Quaternary stratigraphy of the research area can be divided into the Pleistocene (Q_p) and the Holocene (Q_h). The location of stable and continuous low-permeability layers is used as a basis for classifying aquifer groups. The Quaternary aquifers are classified vertically into three main aquifer groups: shallow, medium and deep. Shallow aquifers are mainly phreatic aquifers and, in some areas, also contain relatively shallow pressurized water. The depth of the bottom plate of the shallow aquifer is generally 20 to 40 m. The groundwater in this layer is fed directly by atmospheric precipitation, seepage from rivers and lakes and returned water from agricultural irrigation. For the medium aquifer group, the depth of the lower plate varies from 80 to 120 m. Groundwater from this layer is mainly used for agricultural irrigation in the Chaoyang and Tongzhou regions. This is the group of aquifers with the highest groundwater extraction in the research area. In the western part of the region, the

depth of groundwater in this layer is relatively shallow and recharge is mainly provided by atmospheric precipitation gradually changing to recharge by lateral runoff in the eastern part of the region. For deep aquifers, the depth of the lower plate is between 180 and 250 m and even more than 300 m in some areas. Groundwater recharge is dominated by lateral runoff. Groundwater circulation and renewal are slow. In some suburbs of the Chaoyang, Tongzhou and Daxing districts, groundwater is used mainly by local residents, businesses and institutions for domestic use. The different aquifer layers are presented in Figure 2 through hydrogeologic cross-sections I–I′ and II–II′ [33].

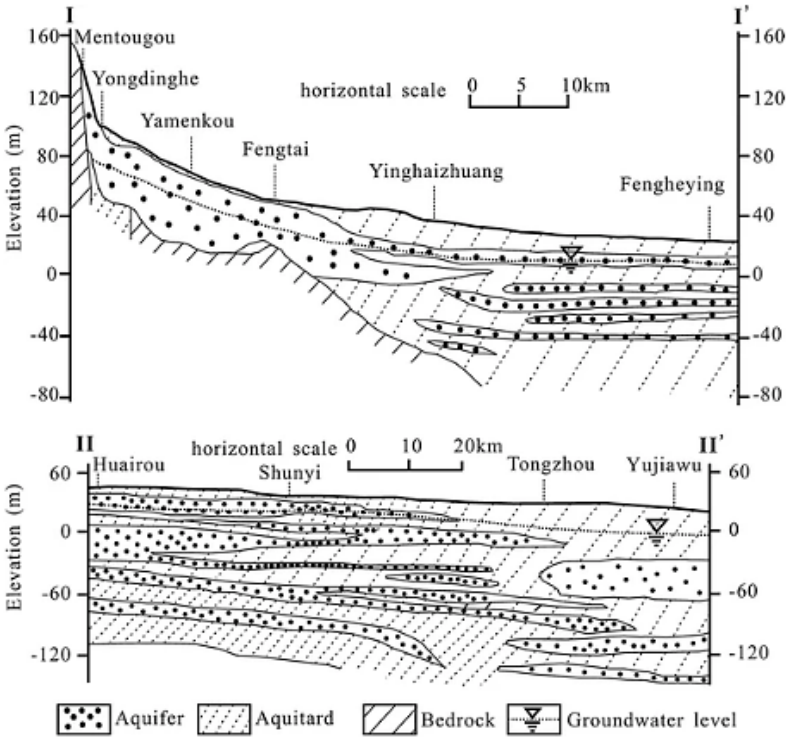

Figure 2. Presentation of hydrogeologic cross sections I∓I′ and II∓II′.

2.3. Groundwater Exploitation and Balance

As illustrated in Figure 3a, Beijing water supply resources are strongly correlated to recharge [34]. In 2007, groundwater was overexploited, accounting for about 70% of total water consumption. In the period from 2007 to 2019, groundwater consumption gradually decreased to 37%. According to the 2020 Beijing Water Resources Bulletin, groundwater volume supply represented a volume of 1.35 billion m^3, accounting for 33.2% of the total water supply (Figure 3b). From 2014, reclaimed water and the South-to-North Water Diversion Project played an important role in the regulation of groundwater exploitation.

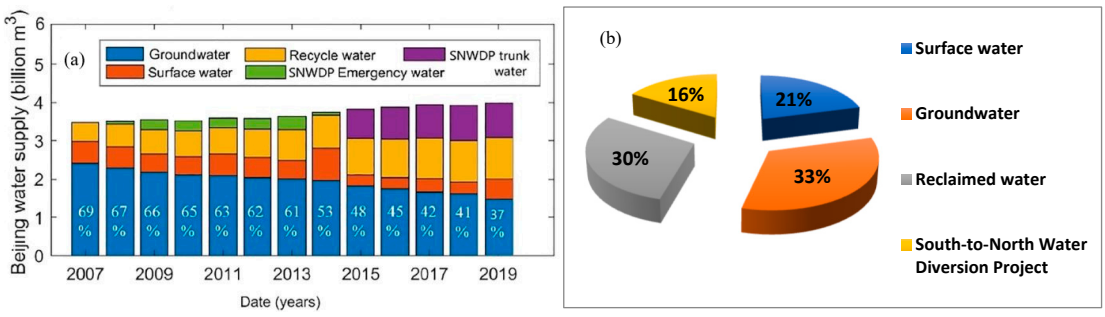

Figure 3. (**a**) Structure of total water resources in Beijing from 2007 to 2019. (**b**) Beijing water supply repartition in 2020.

As shown in Table 1, recharge (mostly from rainfall infiltration) and extraction volumes are estimated, respectively, to have been 1.5 billion and 1.478 billion m^3 in 2020. Evaporation only exists in small areas in very small proportions, so it is not considered.

Table 1. Groundwater recharge and discharge items in the study area (10^8 m^3).

Supply Items		Excretory Item	
Precipitation infiltration amount	10.21	Evaporation	Negligible
River infiltration amount	3.69	Artificial mining	14.78
Irrigation replenishment amount	1.07		

Many scholars established a correlation between groundwater volume changes and quality [35,36]. Through their different studies, they were able to demonstrate the changes in chemical types and ion concentrations in specific areas of the research area.

3. Materials and Methods

3.1. Sample Collection and Testing

To assess the groundwater quality in the quaternary aquifer of the Beijing Plain, samples were collected in 2020 according to the Groundwater Environmental Monitoring Manual (HJ 164–2020). In total, 110 groundwater samples were collected at depths ranging from 30 to 110 m and labeled according to the sampling order. The location and distribution map of sampling points was realized using ArcGIS 10.5 software (Figure 4).

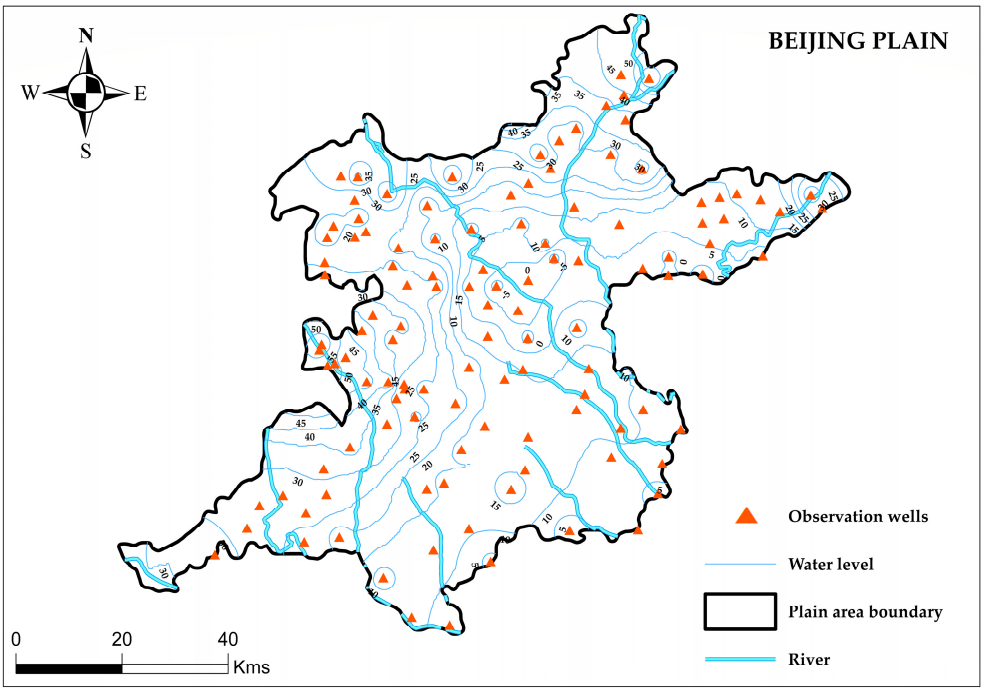

Figure 4. Spatial distribution of the groundwater samples.

Groundwater chemical analysis at the laboratory had been performed for a total of more than 20 selected parameters. Among them, pH, total hardness, total dissolved solids (TDS), ammonium (NH_4^+), potassium (K^+), sodium (Na^+), calcium (Ca^{2+}), magnesium (Mg^{2+}), sulfate (SO_4^{2-}), chloride (Cl^-), bicarbonate (HCO_3^-), iron (Fe^{2+}/Fe^{3+}), nitrite (NO_2^-), nitrate (NO_3^-) and manganese (Mn^{2+}) concentrations were determined.

The anion and cation balance reliability calculations were performed for all laboratory results to ensure the data reliability. The following equation was applied for the calculation:

$$D(\%) = \frac{\sum C_c - \sum C_A}{\sum C_c + \sum C_A} \times 100 \quad (1)$$

where D is the relative error; C_c and C_A are, respectively, cation and anion concentrations in the groundwater sample (meq/L).

The relative error value that resulted from anion and cation balance calculations for all the groundwater samples were between ±5% and the test results were reliable.

3.2. Data Analysis Methods

In this paper, ArcGIS 10.5, Diagrammes, SPSS 27 and PHREEQC 3.7.3 were used for groundwater chemistry characterization. SPSS software was used in this study for the descriptive statistics. In addition, ionic ratios were used to assess the sources of major ions in groundwater and to reveal the main factors controlling geochemical processes. On the other hand, the hydrogeochemical inversion simulations were performed by using PHREEQC software.

3.3. Hydrogeochemical Inversion Simulation Descriptive Method

3.3.1. Selection of Simulation Pathways

The inverse simulation paths of hydrogeochemistry should be selected following the principle that the groundwater samples at the starting and termination points are from upstream to downstream. Therefore, in this paper, four typical pressurized water paths I, II, III and IV were selected along the groundwater flow direction in the research area (Figure 5). Due to years of over-exploitation of groundwater in the research area, a groundwater level descent funnel was formed in the center and north-east parts, especially in the Shunyi and Chaoyang districts, which changed the direction of the groundwater flow and the hydrogeochemical environment. Paths I, II and III of the water flow paths were selected from the north-western parts of the research area, which flowed towards the descent funnel. Path I will be used to study the influence of the water from the Miyun reservoir and Mihuaishun water source activities. Path II and III will be used to study the influence of water from the mountain flow and the third water source and fourth water source activities. Path IV has been selected to research the influence of water infiltration from the mountain zone to the river at the southern limit of the research area towards the Hebei province.

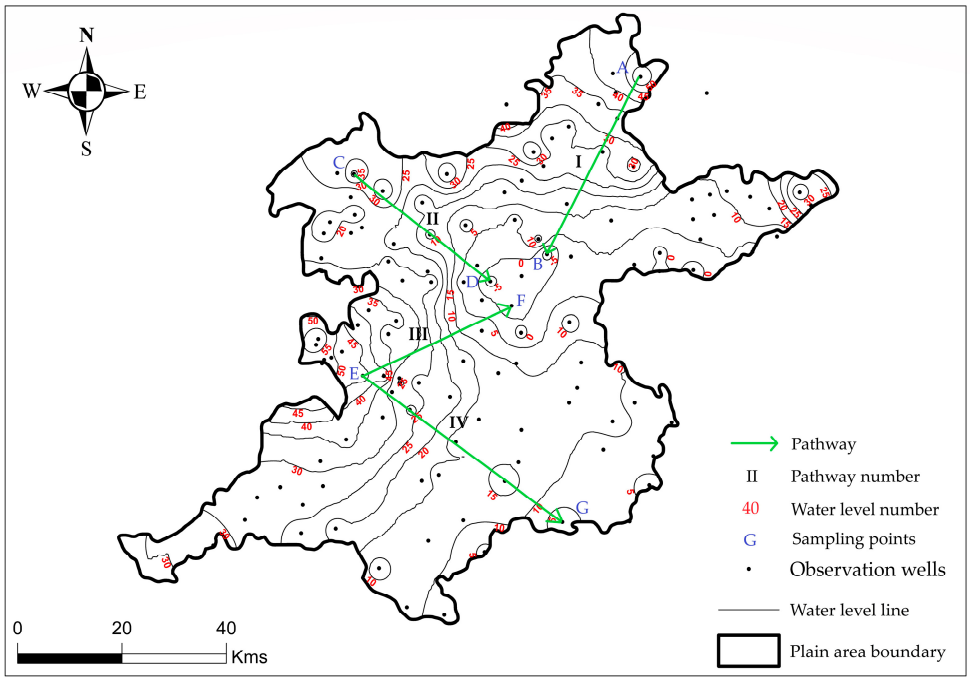

Figure 5. Selected simulation paths.

The hydrogeochemical inverse simulation was carried out based on the selected starting points and the terminating groundwater samples on paths I, II, III and IV. Sampling points labeled A, C, E were selected as upstream and points B, D, F and G as downstream. For the inverse hydrogeochemical simulation performed with PHREEQC software, the groundwater chemical results obtained at these chosen sampling points were used as input data. Iterations were performed depending on the path for uncertainty settings.

3.3.2. Selection of Possible Mineral Phases

Possible mineral phases refer to the mineral and gas components that are directly involved in the water–rock–gas reaction in the groundwater. The lithology of the Quaternary aquifer in the research area is mainly dominated by gravel pebbles and medium-coarse sands, which mainly contain silicate rock salts [37]. The evolution of the groundwater chemical composition in the research area may be affected by the hydrolysis of silicate rock, carbonate rock and sulfate rock [38].

Carbonate rocks (calcite, dolomite), silicate rocks (calcium montmorillonite, potassium feldspar, sodium feldspar, kaolinite), and sulfate rocks (rock salt, gypsum) were selected as possible mineral phases in the model. C, Si, K, Na, Ca Mg, S and Cl were used as constraint variables. Based on an ion relation study, the Ca-Na-Mg cation exchange process was also selected for the simulation. The chemical formulas and reaction equations for the various mineral phases are presented in Table 2 [39].

Table 2. Chemical formulas and reaction equations for possible mineral phases.

Possible Mineral Phases	Chemical Formulas	Reaction Equations
Calcite	$CaCO_3$	$CaCO_3 = Ca^{2+} + CO_3^{2-}$
Dolomite	$CaMg(CO_3)_2$	$CaMg(CO_3)_2 = Ca^{2+} + Mg^{2+} + 2CO_3^{2-}$
Gypsum	$CaSO_4{:}2H_2O$	$CaSO_4{:}2H_2O = Ca^{2+} + SO_4^{2-} + 2H_2O$
Calcium montmorillonite	$Ca_{0.17}Al_{2.33}Si_{3.67}O_{10}(OH)_2$	$6Ca_{0.17}Al_{2.33}Si_{3.67}O_{10}(OH)_2 + 60H_2O + 12OH^- = Ca^{2+} + 14Al(OH)_4^- + 22H_4SiO_4$
Rock salt	NaCl	$NaCl = Na^+ + Cl^-$
Kaolinite	$Al_2Si_2O_5(OH)_4$	$Al_2Si_2O_5(OH)_4 + 6H^+ = H_2O + 2H_4SiO_4 + 2Al^{3+}$
Sodium feldspar	$NaAlSi_3O_8$	$NaAlSi_3O_8 + 8H_2O = Na^+ + Al(OH)_4^- + 3H_4SiO_4$
Potassium feldspar	$KAlSi_3O_8$	$CaAl_2Si_2O_8 + 8H_2O = Ca^{2+} + 2Al(OH)_4^- + 3H_4SiO_4$
Cation exchange	CaX_2 MgX_2 NaX	$Ca^{2+} + 2NaX = 2Na^+ + CaX_2$ $Mg^{2+} + 2NaX = 2Na^+ + MgX$

4. Results and Discussion

4.1. Hydrogeochemical Characteristics

A descriptive statistical analysis (minimum, median, maximum, mean and standard deviation) of the results data of 14 hydrogeochemical parameters of groundwater samples was obtained by using SPSS software (Table 3). The pH varied from 6.76 to 8.65 with an average value of 7.92, and the groundwater was weakly alkaline. The TDS varied from 235 to 1200 mg/L with a mean value of 539.52 mg/L. The overall content was not high, and it was freshwater. According to the records of the sampling points, the groundwater sampling points with high TDS values are mainly located in the Chaoyang and Fentai districts of the research area. The total hardness (TH) of the groundwater could reflect the lithological characteristics of the strata, with concentrations ranging from 51 to 677 mg/L and a mean value of 264.07 mg/L. The order of major cations in groundwater in the research area was $Ca^{2+} > Na^+ > Mg^{2+} > K^+$ with average values of 66.54 mg/L, 50.58 mg/L, 23.78 mg/L, and 1.81 mg/L, respectively. The order of major anions in the groundwater was $HCO_3^- > SO_4^{2-} > Cl^-$ with average values of 284.89 mg/L, 52.1 mg/L and 35.5 mg/L, respectively.

The average concentrations of NO_2^- and NO_3^- were 0.22 and 39.07 mg/L with range values from 0.001–3.98 mg/L and 0.037–157 mg/L, respectively.

Table 3. Statistical results of the hydrogeochemical parameters of groundwater in the research area.

Parameters	Minimum (mg/L)	Median (mg/L)	Maximum (mg/L)	Mean (mg/L)	Standard Deviation (mg/L)
pH	6.760	7.970	8.650	7.919	0.358
K^+	0.110	1.250	5.420	1.806	1.410
Na^+	7.000	50.000	112.000	50.579	30.921
Ca^{2+}	13.800	54.700	171.000	66.537	39.567
Mg^{2+}	3.400	18.750	62.200	23.777	15.842
NH_4^+	0.020	0.185	2.380	0.351	0.482
HCO_3^-	25.600	273.000	503.000	284.887	116.764
Cl^-	0.800	13.800	148.000	35.497	42.076
SO_4^{2-}	1.500	38.350	154.000	52.101	40.488
NO_3^-	0.037	13.300	157.000	39.067	48.391
NO_2^-	0.001	0.022	3.980	0.216	0.669
TH	51.000	215.500	677.000	264.065	159.589
TDS	235.000	438.500	1200.000	539.522	281.933

Note: Statistical analysis was performed on the laboratory results of 110 groundwater samples collected in the study area.

A comparison of the average concentration values obtained according to the indicators was carried out with those presented in the China Groundwater Quality Standards GB/T14848-2017 [40]. Particular attention should be paid to NO_3^-, NH_4^+ ions, TH and TDS, with concentrations exceeding 20 mg/L, 1 mg/L, 450 mg/L and 1000 mg/L, respectively. These parameters' concentrations exceed the values of limit class III, indicating groundwater was identified as being average to poor quality.

4.2. Hydrochemical Types

There are seven anions and cations in groundwater, including chloride ion (Cl^-), sulfate ion (SO_4^{2-}), bicarbonate ion (HCO_3^-), sodium ion (Na^+), potassium ion (K^+), calcium ion (Ca^{2+}) and magnesium ion (Mg^{2+}). These anions and cations can reflect the mechanism of the formation of the chemical composition of groundwater and identify the hydrochemical information of groundwater by the construction and study of a Piper's trilinear diagram [41–43] (Figure 6). The monitoring wells in the research area were divided into three groups: Miyun reservoir wells, south-to-north water project wells and the other observation wells in the Beijing Plain area. In the cation triangulation diagram, the distribution of groundwater sample points is relatively scattered. Most of them are concentrated in the Ca-Na-Mg region, indicating mixed-type water. The content of each cation is more uniform, and Ca^{2+}, Na^+ and Mg^{2+} are the dominant cations. A few samples were found to be located in zones A and D with calcium Ca^{2+} and sodium Na^+ ions dominating, respectively. Most of the groundwater in the Miyun reservoir and south-to-north project observation wells is calcic. In the anion triangulation diagram, the sample points are mostly located in zone E, and HCO_3^- is the dominant anion in the groundwater of the research area, reflecting the dissolution of carbonate minerals. Some samples are located in the HCO_3-Cl-SO_4 region (zone B), indicating mixed-type water. In the middle diamond-shaped chart area, the dominant types of groundwater geochemistry are Mg-Ca-Cl-HCO_3, Na-Ca- HCO_3, Mg-Ca-HCO_3 and Mg-Na-HCO_3. The majority of samples are of Ca-HCO_3 type and located in zone 1.

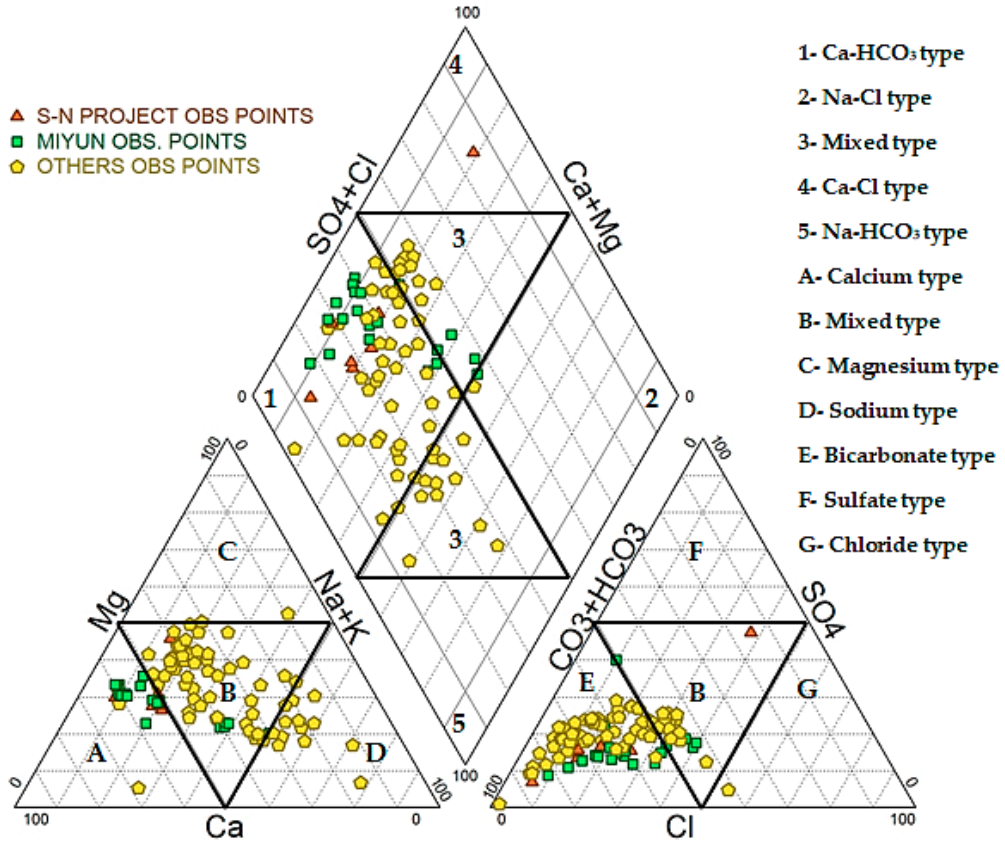

Figure 6. Piper trilinear diagram for groundwater samples.

4.3. Main Control Factors and Sources of Water Chemistry

4.3.1. Gibbs Plots

Gibbs plots are commonly used to reflect the controlling factors of major ions in groundwater on a macroscopic scale and to qualitatively determine the source of water chemistry [43]. Based on the ratios of $Na^+/(Na^+ + Ca^{2+})$ and $Cl^-/(Cl^- + HCO_3^-)$ to TDS, respectively, the Gibbs diagram is divided into three dominant zones: rock weathering dominant zone, evaporation concentration dominant zone and atmospheric precipitation dominant zone (Figure 7). The ratio of $Na^+/(Na^+ + Ca^{2+})$ is between 0.1 and 0.9, and the TDS value does not change with the ratio of $Na^+/(Na^+ + Ca^{2+})$, which indicates that the other controlling factors do not have a significant effect on the cations in the groundwater. Because groundwater remains in the aquifer for a much longer time than surface water, it is subject to water–rock interactions for a long period of time. The groundwater sampling points in the research area are basically located in the control zone of water–rock interactions, and there are no sample points in the evapotranspiration and atmospheric precipitation zones. The ratio of $Cl^-/(Cl^- + HCO_3^-)$ is between 0 and 0.6, the TDS value changes with the increase in $Cl^-/(Cl^- + HCO_3^-)$) ratio, and groundwater anions were influenced by control factors other than rock weathering. Most of the groundwater sample positions indicated that rock weathering is the main source controlling the evolution of water chemistry and hydrogeochemistry. Some sample points are not located in any control zone, which may be affected by human activities.

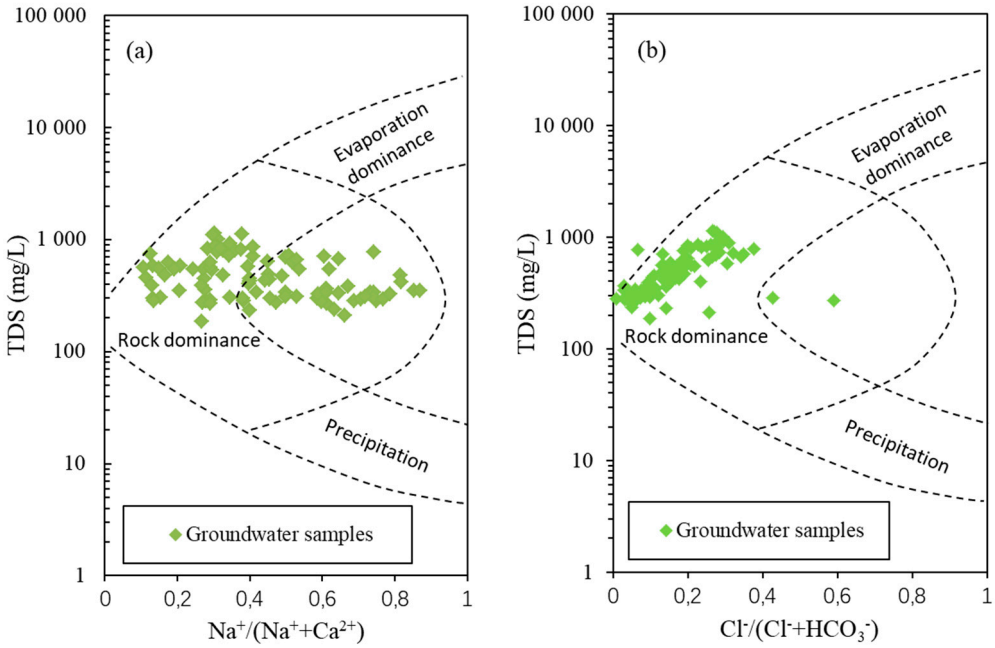

Figure 7. Gibbs diagrams of groundwater in the research area. (**a**) Ratio of $Na^+/(Na^+ + Ca^{2+})$ to TDS. (**b**) Ratio of $Cl^-/(Cl^- + HCO_3^-)$ to TDS.

4.3.2. Ions Ratio Diagram

Hydrogeochemical processes such as water–rock interactions, evaporation and cation exchange play an important role in shaping groundwater chemistry. For example, silicate weathering generally produces Ca^{2+}, K^+, Na^+, Mg^{2+}, HCO_3^- and Si. Carbonate rock weathering produces HCO_3^-, Ca^{2+} and Mg^{2+}, and evaporation and concentration mainly produce SO_4^{2-}, Cl^-, Ca^{2+}, K^+, Na^+ and Mg^{2+}. Ion ratio diagrams are used to research the sources of major ions in groundwater and to reveal the main factors controlling geochemical processes.

Salt rock is a common evaporation rock, and its dissolution releases equal amounts of Na^+ and Cl^-. The graph of the ratio between the equivalent concentrations of these parameters shows groundwater samples distributed on the upper and lower sides of the y = x relationship line (Figure 8a). Na^+ in groundwater does not originate entirely from the dissolution of salt rocks but may also come from other sodium-bearing minerals or from cation exchange. Regarding the ion ratio of the equivalent concentration of $Ca^{2+} + Mg^{2+}$ to $HCO_3^- + SO_4^{2-}$, the groundwater samples are mainly located below the y = x relationship line, indicating that weathering of carbonate and silicate rocks is a factor affecting the geochemistry of the research area (Figure 8b).

The ratio of the equivalent concentration of Ca^{2+} to HCO_3^- is presented in Figure 8c to determine the dissolution equilibrium of carbonate rocks. The groundwater samples are distributed on the upper side of the y = x relationship line. Ca^{2+} in groundwater, in addition to originating from calcite dissolution, may originate from cation exchange or from the saturation or precipitation of certain carbonate minerals that consume HCO_3^-. SO_4^{2-} in groundwater can result from the dissolution of gypsum. As shown in Figure 8d, the ratio of equivalent Ca^{2+} and SO_4^{2-} concentrations lies below the line of the y = x relationship, indicating an equivalent concentration of Ca^{2+} higher than the equivalent concentration of SO_4^{2-}. Based on the previous statements and mineral composition, this result may be due to the dissolution of associated minerals, such as calcite and dolomite, in the groundwater environment.

The equivalent concentration ratio of Ca^{2+} to Mg^{2+} lies between the y = x and y = 0.5x relationship lines (Figure 9a), suggesting that calcite dissolution is the main process affecting the hydrogeochemical characteristics of groundwater in the study area. Very few

groundwater samples fall below the y = 0.5x relationship line, indicating that they are rarely influenced by silicate weathering. The linear relationship of the graphs of the equivalent concentration ratio of (Ca^{2+} + Mg^{2+})–(HCO_3^- + SO_4^{2-}) and (Na^+–Cl^-) have a linear fitting equation of y = −0.5664x + 0.6237 (Figure 9b). The fitting line slope of −0.7219 close to −1 suggests that a reverse ion exchange is occurring between Na^+ and Ca^{2+} + Mg^{2+}.

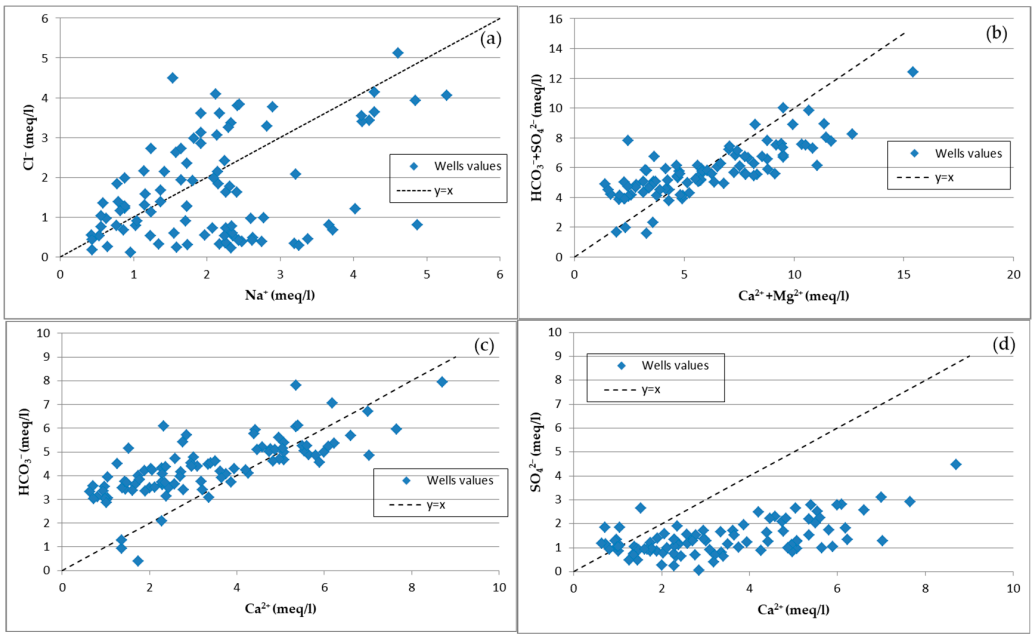

Figure 8. Ion ratio diagrams in groundwater. (**a**) Diagram of Cl^- vs. Na^+. (**b**) Diagram of (SO_4^{2-} + HCO_3^-) vs. (Ca^{2+} +Mg^{2+}). (**c**) Diagram of HCO_3^- vs. Ca^{2+}. (**d**) Diagram of SO_4^{2-} vs. Ca^{2+}.

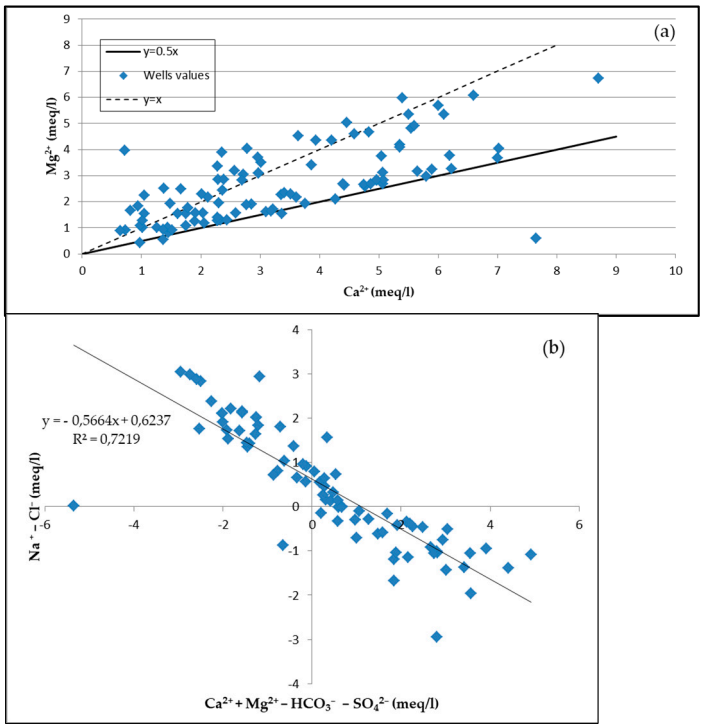

Figure 9. Ion ratio diagrams in groundwater. (**a**) Diagram of Mg^{2+} vs. Ca^{2+}. (**b**) Diagram of (Ca^{2+} + Mg^{2+}–HCO_3^-–SO_4^{2-}) vs. (Na^+–Cl^-).

4.4. Inverse Hydrogeochemical Simulation Results

The inverse simulation results of the hydrogeochemical study conducted using PHREEQC according to each of the four selected pathways are presented in Table 4.

Table 4. Inverse simulation results of groundwater hydrogeochemistry.

Possible Mineral Phases	Chemical Formulas	Reaction Paths Results			
		Path I	Path II	Path III	Path IV
Calcite	$CaCO_3$	-	-	-	-
Calcium montmorillonite	$CaMg(CO_3)_2$	6.59×10^{-3}	-5.72×10^{-3}	1.19×10^{-2}	7.86×10^{-3}
Dolomite	$CaSO_4{:}2H_2O$	9.84×10^{-3}	-7.87×10^{-4}	9.26×10^{-4}	1.30×10^{-3}
Gypsum	$Ca_{0.17}Al_{2.33}Si_{3.67}O_{10}(OH)_2$	9.25×10^{-5}	3.94×10^{-4}	4.73×10^{-4}	3.56×10^{-6}
Rock salt, Halite	NaCl	3.98×10^{-4}	9.87×10^{-4}	6.23×10^{-4}	-3.31×10^{-4}
Kaolinite	$Al_2Si_2O_5(OH)_4$	-5.47×10^{-3}	4.45×10^{-3}	-9.85×10^{-3}	-6.52×10^{-3}
Potassium feldspar	$NaAlSi_3O_8$	-2.10×10^{-5}	3.87×10^{-5}	-2.68×10^{-5}	-3.32×10^{-5}
Sodium feldspar	$KAlSi_3O_8$	-4.40×10^{-3}	3.80×10^{-3}	-7.93×10^{-3}	-5.23×10^{-3}
Cation exchange	CaX_2	-2.38×10^{-3}	1.58×10^{-3}	-3.59×10^{-3}	-2.67×10^{-3}
	MgX_2	-7.17×10^{-4}	1.60×10^{-3}	-1.12×10^{-3}	-1.31×10^{-3}
	NaX	6.19×10^{-3}	-6.35×10^{-3}	9.43×10^{-3}	7.95×10^{-3}

Note: Positive values indicate migration into the solution (dissolution), negative values indicate migration out of the solution (precipitation) and "-" indicates no relevant results.

Path I mainly undergoes the dissolution of calcium montmorillonite, dolomite and rock salt, dissolving 6.592×10^{-3} mmol/LH_2O, 9.840×10^{-3} and 3.975×10^{-4} mmol/LH_2O, respectively. The cation exchange that occurs in this path is mainly due to the adsorption of 6.191×10^{-3} mmol/LH_2O on Na^+ and release of Ca^{2+} and Mg^{2+} into the groundwater through the mineral medium, flowing along the way with release amounts of 2.379×10^{-3} mmol/LH_2O and 7.167×10^{-4} mmol/LH_2O, respectively. Gypsum is also dissolved with the amount of 9.246×10^{-5} mmol/LH_2O.

The ion exchange interaction in path II is described by the adsorption of Ca^{2+}, Mg^{2+} in 1.576×10^{-3} mmol/LH_2O, 1.598×10^{-3} mmol/LH_2O, respectively, and the release of Na^+ in 6.348×10^{-3} mmol/LH_2O. Due to the dissolution of rock salt and gypsum in this pathway with respective precipitation amounts of 9.87×10^{-4} mmol/LH_2O and 3.939×10^{-4} mmol/LH_2O, an increase in Cl^- and $SO_4{}^{2-}$ concentrations was noticed.

The groundwater in pathway III mainly undergoes adsorption of gypsum and rock salt with 4.726×10^{-4} mmol/LH_2O and 6.229×10^{-4} mmol/LH_2O. The cation exchange that occurs in this path is mainly due to the adsorption of 9.431×10^{-3} mmol/LH_2O on Na^+ and release of Ca^{2+} and Mg^{2+} at amounts of 3.593×10^{-3} mmol/LH_2O and 1.122×10^{-4} mmol/LH_2O, respectively. Dolomite with 9.26×10^{-3} mmol/LH_2O is also absorbed.

Groundwater in pathway IV mainly undergoes leaching and filtration processes of silicate and carbonate rocks. Ca Na and Mg Na undergo ion exchange, with the aquifer medium absorbing 2.668×10^{-3} mmol/LH_2O and 1.309×10^{-3} mmol/LH_2O, respectively. Na^+ of 7.954×10^{-3} mmol/LH_2O enters groundwater from the aquifer medium, and rock salt precipitates 3.308×10^{-4} mmol/LH_2O.

The analysis of the inverse simulation results carried out using the PHREEQC software indicates that the hydrogeochemical changes observed in the research area are consistent with the results of the groundwater chemical analysis obtained. The dissolution of carbonate rocks (dolomite), sulfate rocks (gypsum, rock salt) and silicate rocks (sodium feldspar, potassium feldspar) influenced the hydrogeochemical characteristics of groundwater.

5. Conclusions

For this research, 110 groundwater samples were collected and analyses were performed by using statistics, water chemistry, and hydrogeochemical simulation methods to

determine groundwater chemical characteristics in the Beijing Plain. The main conclusions drawn from this study are as follows:

(1) The pH results indicated weakly alkaline groundwater in Beijing Plain aquifers. The order of major cations and anions in the groundwater of the research area were Ca^{2+} > Na^{+} > Mg^{2+} > K^{+} and HCO_3^{-}> SO_4^{2-}> Cl^{-}, respectively.

(2) Based on the anions and cations distribution in groundwater and Piper's trilinear diagram study, the dominant water chemistry types were Mg-Ca-Cl-HCO_3, Na-Ca- HCO_3, Mg-Ca-HCO_3 and Mg-Na-HCO_3. The majority of samples were Ca-HCO_3 type.

(3) The main factors affecting groundwater chemistry are related to the dissolution of minerals and some human activities in the region. Gibbs plots and ion ratios results indicated that silicate and carbonate rock weathering, as well as cation adsorption (Na^{+}, Ca^{2+} and Mg^{2+}) were the main elements affecting the hydrogeochemical characteristics of the Quaternary aquifer in the research area.

(4) Inverse hydrogeochemical simulation results indicated that changes observed in the research area are consistent with previous results obtained by water geochemistry analysis methods. The hydrogeochemical characteristics of the groundwater of the Beijing Plain were influenced by the dissolution of carbonate minerals (dolomite), sulfate minerals (gypsum, rock salt) and silicate rocks (calcium montmorillonite, sodium feldspar, potassium feldspar). The ion concentrations vary according to the water flow, the path length, and upstream and downstream points.

In conclusion, the various results showed that the quality of the groundwater in the aquifers of the Quaternary zone of the study area is relatively good, with the exception of a few places where the parameters studied exceed the Chinese standard values for groundwater. These areas need to be monitored more closely, and groundwater management and decision-making will be better guided by this type of investigation. The study of the impact of the continuous abstraction and the future increase in the abstraction on the groundwater quality with time through numerical simulation is suggested for an advanced comprehension of groundwater quality evolution in the Beijing Plain.

Author Contributions: Conceptualization Y.Z.; methodology, Y.Z.; software, S.F.C.; validation, J.Z.; formal analysis, S.F.C., J.Z.; investigation, S.F.C.; resources, Y.Z.; data curation, S.F.C.; writing—original draft preparation, S.F.C.; writing—review and editing, J.Z. All authors have read and agreed to the published version of the manuscript.

Funding: This work was supported by the Beijing Natural Science Foundation [8242003]; Open Research Fund Program of State key Laboratory of Hydroscience and Engineering [sklhse-2024-C-03]; Major Science and Technology Innovation Pilot Project for Water Resources Protection and Integrated-Saving Utilization in the Yellow River Basin of the Inner Mongolia Autonomous Region [grant number: No. 2023JBGS0007]; R&D Program of Beijing Municipal Education Commission [grant number: KM202310005023 & KM202210005017]. Common Prosperity and Corporate ESG: Theoretical Modeling and Empirical Research [FRG-23-029-MSB].

Data Availability Statement: The data presented in this study are available upon request from the corresponding author.

Conflicts of Interest: The authors declare no conflicts of interest.

References

1. Kılıç, Z. The importance of water and conscious use of water. *Int. J. Hydrol.* **2020**, *4*, 239–241. [CrossRef]
2. Hossain, M. WATER: THE MOST PRECIOUS RESOURCE OF OUR LIFE. *Glob. J. Adv. Res.* **2015**, *2*, 1436–1445.
3. Frappart, F.; Merwade, V.M. Editorial: Groundwater systems worldwide. *Front. Earth Sci.* **2022**, *10*, 1097789. [CrossRef]
4. Zhao, S.; Zhou, D.; Zhu, C.; Qu, W.; Zhao, J.; Sun, Y.; Huang, D.; Wu, W.; Liu, S. Rates and patterns of urban expansion in China's 32 major cities over the past three decades. *Landsc. Ecol.* **2015**, *30*, 1541–1559. [CrossRef]
5. Yang, L.; Tian, F.; Smith, J.A.; Hu, H. Urban signatures in the spatial clustering of summer heavy rainfall events over the Beijing metropolitan region. *J. Geophys. Res. Atmos.* **2014**, *119*, 1203–1217. [CrossRef]
6. Liu, J.; Yang, H.; Savenije, H.H.G. China's move to higher-meat diet hits water security. *Nature* **2008**, *454*, 397. [CrossRef]

7. Wang, J.; Shang, Y.; Wang, H.; Zhao, Y.; Yin, Y. Beijing's Water Resources: Challenges and Solutions. *JAWRA J. Am. Water Resour. Assoc.* **2015**, *51*, 614–623. [CrossRef]
8. Qian, L.; Zhang, R.; Hong, M.; Wang, H.; Yang, L. A new multiple integral model for water shortage risk assessment and its application in Beijing, China. *Nat. Hazards* **2016**, *80*, 43–67. [CrossRef]
9. *Beijing Water Resource Bulletin (1999–2015)*; Beijing Water Authority: Beijing, China, 2015.
10. Jie, L.; Zheng, C. Towards Integrated Groundwater Management in China. In *Integrated Groundwater Management: Concepts, Approaches and Challenges*; Jakeman, A.J., Barreteau, O., Hunt, R.J., Rinaudo, J.-D., Ross, A., Eds.; Springer International Publishing: Cham, Switzerland, 2016. [CrossRef]
11. Zhang, J.; Zhou, J.; Zhou, Y.; Zeng, Y.; Ji, Y.; Sun, Y.; Lei, M. Hydrogeochemical characteristics and groundwater quality assessment in the plain area of Yarkant River Basin in Xinjiang, P.R. China. *Environ. Sci. Pollut. Res.* **2021**, *28*, 31704–31716. [CrossRef]
12. Liu, F.; Wang, S.; Wang, L.; Shi, L.; Song, X.; Yeh, T.-C.J.; Zhen, P. Coupling hydrochemistry and stable isotopes to identify the major factors affecting groundwater geochemical evolution in the Heilongdong Spring Basin, North China. *J. Geochem. Explor.* **2019**, *205*, 106352. [CrossRef]
13. Ren, X.; Li, P.; He, X.; Su, F.; Elumalai, V. Hydrogeochemical Processes Affecting Groundwater Chemistry in the Central Part of the Guanzhong Basin, China. *Arch. Environ. Contam. Toxicol.* **2021**, *80*, 74–91. [CrossRef]
14. Sun, H.; Bian, K.; Wang, T.; Jin, Z.; Niu, Z. Hydrogeochemical Characteristics and Genetic Analysis of Karst Groundwater in the Fengfeng Mining Area. *Water* **2023**, *15*, 4049. [CrossRef]
15. Wang, S.; Chen, J.; Jiang, W.; Zhang, S.; Jing, R.; Yang, S. Identifying the geochemical evolution and controlling factors of the shallow groundwater in a high fluoride area, Feng County, China. *Environ. Sci. Pollut. Res.* **2023**, *30*, 20277–20296. [CrossRef] [PubMed]
16. Bozdağ, A. Assessment of the hydrogeochemical characteristics of groundwater in two aquifer systems in Çumra Plain, Central Anatolia. *Environ. Earth Sci.* **2016**, *75*, 674. [CrossRef]
17. Xing, L.; Guo, H.; Zhan, Y. Groundwater hydrochemical characteristics and processes along flow paths in the North China Plain. *J. Asian Earth Sci.* **2013**, *70–71*, 250–264. [CrossRef]
18. Wang, R.; Bian, J.-M.; Gao, Y. Research on hydrochemical spatio-temporal characteristics of groundwater quality of different aquifer systems in Songhua River Basin, eastern Songnen Plain, Northeast China. *Arab. J. Geosci.* **2014**, *7*, 5081–5092. [CrossRef]
19. Ren, C.; Zhang, Q. Groundwater Chemical Characteristics and Controlling Factors in a Region of Northern China with Intensive Human Activity. *Int. J. Environ. Res. Public Health* **2020**, *17*, 9126. [CrossRef] [PubMed]
20. Gogoi, R.R.; Khanikar, L.; Gogoi, J.; Neog, N.; Deka, D.J.; Sarma, K.P. Geochemical sources, hydrogeochemical behaviour of fluoride release and its health risk assessment in some fluorosis endemic areas of the Brahmaputra valley of Assam, India. *Appl. Geochem.* **2021**, *127*, 104911. [CrossRef]
21. Fuchu, Z.; Bin, W.; Fan, G.; Mingliang, D.; Liantong, X. Hydrochemical characteristics of groundwater and evaluation of water quality in arid area of Northwest China: A case study in the plain area of Kuitun River Basin. *Arab. J. Geosci.* **2021**, *14*, 2099. [CrossRef]
22. Papatheodorou, G.; Demopoulou, G.; Lambrakis, N. A long-term study of temporal hydrochemical data in a shallow lake using multivariate statistical techniques. *Ecol. Model.* **2006**, *193*, 759–776. [CrossRef]
23. Parkhurst, D.L.; Appelo, C.A.J. User's guide to PHREEQC (Version 2): A Computer Program for Speciation, Batch-Reaction, One-Dimensional Transport, and Inverse Geochemical Calculations. In *Water-Resources Investigations Report*; Report 99-4259; 1999. Available online: https://pubs.usgs.gov/publication/wri994259 (accessed on 23 March 2024).
24. Xie, X.; Wang, Y.; Li, J.; Su, C.; Duan, M. Hydrogeochemical and Isotopic Investigations on Groundwater Salinization in the Datong Basin, Northern China. *JAWRA J. Am. Water Resour. Assoc.* **2013**, *49*, 402–414. [CrossRef]
25. Huang, L.; Sun, Z.; Zhou, A.; Bi, J.; Liu, Y. Source and enrichment mechanism of fluoride in groundwater of the Hotan Oasis within the Tarim Basin, Northwestern China. *Environ. Pollut.* **2022**, *300*, 118962. [CrossRef] [PubMed]
26. Jia, Y.; Xi, B.; Jiang, Y.; Guo, H.; Yang, Y.; Lian, X.; Han, S. Distribution, formation and human-induced evolution of geogenic contaminated groundwater in China: A review. *Sci. Total Environ.* **2018**, *643*, 967–993. [CrossRef] [PubMed]
27. Guo, L.; Gong, H.; Zhu, F.; Zhu, L.; Zhang, Z.; Zhou, C.; Gao, M.; Sun, Y. Analysis of the Spatiotemporal Variation in Land Subsidence on the Beijing Plain, China. *Remote Sens.* **2019**, *11*, 1170. [CrossRef]
28. Chen, B.; Gong, H.; Chen, Y.; Li, X.; Zhou, C.; Lei, K.; Zhu, L.; Duan, L.; Zhao, X. Land subsidence and its relation with groundwater aquifers in Beijing Plain of China. *Sci. Total Environ.* **2020**, *735*, 139111. [CrossRef] [PubMed]
29. Zhou, Y.; Xiao, W.; Wang, J.; Zhao, Y.; Huang, Y.; Tian, J.; Chen, Y. Evaluating Spatiotemporal Variation of Groundwater Depth/Level in Beijing Plain, a Groundwater-Fed Area from 2001 to 2010. *Adv. Meteorol.* **2016**, *2016*, 8714209. [CrossRef]
30. Wanshun, W. *Beijing Urban Geological Atlas*; China Earth Press: Beijing, China, 2008.
31. *Beijing Regional Geological Journal*; Beijing Geological Survey Research Institute: Beijing, China, 2018.
32. Gao, Z. Introduction to "Geology Cloud 3.0"-National Earth Science Big Data Shared Service Platform. *China Geol.* **2022**, *49*, 2.
33. Zhai, Y.; Wang, J.; Teng, Y.; Zuo, R. Hydrogeochemical and isotopic evidence of groundwater evolution and recharge in aquifers in Beijing Plain, China. *Environ. Earth Sci.* **2013**, *69*, 2167–2177. [CrossRef]
34. Du, Z.; Ge, L.; Ng, A.H.-M.; Lian, X.; Zhu, Q.; Horgan, F.G.; Zhang, Q. Analysis of the impact of the South-to-North water diversion project on water balance and land subsidence in Beijing, China between 2007 and 2020. *J. Hydrol.* **2021**, *603*, 126990. [CrossRef]

35. He, Z.; Han, D.; Song, X.; Yang, L.; Zhang, Y.; Ma, Y.; Bu, H.; Li, B.; Yang, S. Variations of Groundwater Dynamics in Alluvial Aquifers with Reclaimed Water Restoring the Overlying River, Beijing, China. *Water* **2021**, *13*, 806. [CrossRef]
36. Zhang, Y.; Yu, Y. Evaluating the impact of percolated reclaimed water from river-channel reservoir on groundwater using tracers in Beijing, Northern China. *Environ. Earth Sci.* **2021**, *80*, 138. [CrossRef]
37. Liu, Y.; Wu, Q.; Lin, P.; Liu, J.; Xing, L.; Gao, Z. Restudy of the storage and migration model of the Quaternary groundwater in Beijing Plain area. *Sci. China Earth Sci.* **2012**, *55*, 1147–1158. [CrossRef]
38. Bai, X.; Tian, X.; Li, J.; Wang, X.; Li, Y.; Zhou, Y. Assessment of the Hydrochemical Characteristics and Formation Mechanisms of Groundwater in A Typical Alluvial-Proluvial Plain in China: An Example from Western Yongqing County. *Water* **2022**, *14*, 2395. [CrossRef]
39. Jiang, B.; Gao, J.; Du, K.; Deng, X.; Zhang, K. Insight into the water–rock interaction process and purification mechanism of mine water in underground reservoir of Daliuta coal mine in China. *Environ. Sci. Pollut. Res.* **2022**, *29*, 28538–28551. [CrossRef] [PubMed]
40. Standard for Groundwater Quality GB/T 14848-2017, China, 2017. Available online: https://www.hhtz.gov.cn/art/2023/6/12/art_1229731480_4172921.html (accessed on 12 February 2024).
41. Piper, A.M. A graphic procedure in the geochemical interpretation of water-analyses. *Eos Trans. Am. Geophys. Union* **1944**, *25*, 914–928.
42. Li, C.; Gao, Z.; Chen, H.; Wang, J.; Liu, J.; Li, C.; Teng, Y.; Liu, C.; Xu, C. Hydrochemical analysis and quality assessment of groundwater in southeast North China Plain using hydrochemical, entropy-weight water quality index, and GIS techniques. *Environ. Earth Sci.* **2021**, *80*, 523. [CrossRef]
43. Gao, Z.; Han, C.; Yuan, S.; Liu, J.; Peng, Y.; Li, C. Assessment of the hydrochemistry, water quality, and human health risk of groundwater in the northwest of Nansi Lake Catchment, north China. *Environ. Geochem. Health* **2022**, *44*, 961–977. [CrossRef]